

Low-field mobility spectrum in nonparabolic compound semiconductors

This article has been downloaded from IOPscience. Please scroll down to see the full text article.

2004 J. Phys.: Condens. Matter 16 8267

(<http://iopscience.iop.org/0953-8984/16/46/013>)

View [the table of contents for this issue](#), or go to the [journal homepage](#) for more

Download details:

IP Address: 129.252.86.83

The article was downloaded on 27/05/2010 at 19:06

Please note that [terms and conditions apply](#).

Low-field mobility spectrum in nonparabolic compound semiconductors

E Starikov^{1,3}, P Shiktorov¹, V Gružinskis¹, L Reggiani², L Varani³,
J C Vaissière³ and C Palermo³

¹ Semiconductor Physics Institute, A Goštauto 11, 2600 Vilnius, Lithuania

² INFN—National Nanotechnology Laboratory, Dipartimento di Ingegneria dell' Innovazione, Università di Lecce, Via Arnesano s/n, 73100 Lecce, Italy

³ CEM2—Centre d'Electronique et de Micro-optoélectronique de Montpellier (CNRS UMR 5507), Université Montpellier II, 34095 Montpellier Cedex 5, France

Received 8 July 2004, in final form 29 September 2004

Published 5 November 2004

Online at stacks.iop.org/JPhysCM/16/8267

doi:10.1088/0953-8984/16/46/013

Abstract

The low-field mobility spectrum and related quantities is calculated for a nonparabolic band by using the exact solution of the linearized Boltzmann transport equation within the relaxation time approach. Numerical calculations are applied to bulk nitrides at different lattice temperatures and impurity concentrations.

1. Introduction

The comparison between measured characteristics and microscopic theoretical models forms the basis of any expert evaluation and control of semiconductor materials and technology. The lack of a detailed knowledge of the transport and optical properties as well as of the parameters entering the physical models of new materials such as nitrides, carbides, sulfides, etc, has stimulated the development of theoretical tools able to properly account for various details of the band structure, peculiarities of the scattering mechanisms, etc. For this reason, several numerical and analytical approaches have been developed and/or implemented to calculate the relevant measurable parameters of low-field electrical transport, such as carrier mobility and Hall factor as functions of the lattice temperature, doping level, compensation ratio, etc. Among these approaches we recall the Monte Carlo (MC) method [1, 2], the variational principle [3], the iterative technique [4, 5] and the exact solution of the linearized Boltzmann transport equation (LBTE) [6, 7]. Even if the MC method emerges as the most powerful technique, it has the drawback of being computationally very expensive, especially when applied to low-field conditions. Therefore, analytically based approaches are usually introduced for low-field calculations.

For microwave and optoelectronic applications of new materials, the estimation of high-frequency behaviour of their kinetic coefficients is of mandatory importance. In the case of

low-field mobility, this estimate can be performed by iterative techniques [8]. However, from the computational point of view, a drawback of this technique is that all calculations must be repeated for each frequency value. From this point of view, an approach based on the exact solution of the LBTE seems to be preferable since by providing the relaxation time as function of carrier energy it allows one to obtain at once also the frequency dependence of the mobility and, hence, the spectral density of velocity fluctuations by using the Einstein relation. However, the available versions of this approach [6, 7] were developed for the static case and within the simple parabolic band model only.

The aim of the present work is to implement the LBTE approach to the more general case of a nonparabolic (but still spherically symmetric) band model as well as to account for the frequency dependence. The main advantages of the approach are illustrated by numerical calculations performed for the case of electrons in wurtzite GaN and InN which are considered nowadays as promising materials for various microwave and optoelectronic applications (see, e.g. [9] and references therein).

2. Theory

The theoretical procedure is similar to that described in [6, 7]; therefore, below we will only emphasize the main steps. The LBTE for the distribution function $f(\mathbf{p})$ in the presence of a weak static electric field E takes the form [6, 7]

$$e\mathbf{E}\mathbf{v}(\mathbf{p})\frac{d}{d\varepsilon}f_0(\varepsilon) = S[f] = -f(\mathbf{p})\int W(\mathbf{p}, \mathbf{p}')d\mathbf{p}' + \int f(\mathbf{p}')W(\mathbf{p}', \mathbf{p})d\mathbf{p}' \quad (1)$$

where e , \mathbf{p} , $\mathbf{v} = d\varepsilon/d\mathbf{p}$ and ε are, respectively, electron charge, momentum, velocity and energy, $W(\mathbf{p}', \mathbf{p})$ is the transition probability per unit time from state \mathbf{p}' to state \mathbf{p} , and $f_0(\varepsilon)$ the distribution function in thermal equilibrium (for simplicity we consider here nondegenerate statistics only). We restrict ourselves to the case of a spherically symmetric approximation of the conduction band $\varepsilon(\mathbf{p}) = \varepsilon(|\mathbf{p}|)$, when the transition probability is determined by the change of momentum associated with a scattering event $W(\mathbf{p}', \mathbf{p}) = W(\mathbf{p} - \mathbf{p}')$. The latter allows for the collisional term in the right-hand side of equation (1) to be reduced to the scalar relaxation time approximation as

$$S[f] = \frac{f(\mathbf{p}) - f_0(\varepsilon)}{\tau(\varepsilon)} \quad (2)$$

where the relaxation time $\tau(\varepsilon)$ depends on the carrier energy ε only. In the framework of the relaxation time approximation of the collisional term given by equation (2), from equation (1) one obtains the distribution function in the form

$$f(\mathbf{p}) = f_0(\varepsilon) - e\mathbf{E}\mathbf{v}(\mathbf{p})\tau(\varepsilon)\frac{d}{d\varepsilon}f_0(\varepsilon). \quad (3)$$

We remark that in the general case $\tau(\varepsilon)$ is an unknown function to be determined for a given set of scattering mechanisms. To obtain the energy dependence of $\tau(\varepsilon)$ we use the reverse procedure based on the substitution of equation (3) into (1). As a result we obtain an integral equation in the form

$$\sum_k \int W_k(\mathbf{p} - \mathbf{p}') \left[\tau[\varepsilon(\mathbf{p})] - \frac{v(\mathbf{p}') \cos \theta}{v(\mathbf{p})} \tau[\varepsilon(\mathbf{p}')] \frac{f_0[\varepsilon(\mathbf{p}')] }{f_0[\varepsilon(\mathbf{p})]} \right] d\mathbf{p}' = 1 \quad (4)$$

where θ is the angle between \mathbf{p} and \mathbf{p}' and the sum is performed over all scattering mechanisms. For elastic scatterings (ionized and neutral impurities, deformation and piezoelectric acoustic phonons, etc) equation (4) takes the simple form

$$\tau(\varepsilon) \sum_k \int W_k(\mathbf{p} - \mathbf{p}') [1 - \cos \theta] d\mathbf{p}' = 1 \quad (5)$$

which corresponds to the usual Matthiessen rule and allows one to introduce separate contributions related to various elastic scatterings (in principle, the same also holds for deformation optical phonons, since the average of $\cos \theta$ gives zero). For the polar optical phonon with energy $\hbar\omega_0$ the scatterings from the state \mathbf{p} can be combined with this term while the scatterings to the state \mathbf{p} involve values of the relaxation time at another energy $\tau(\varepsilon \pm \hbar\omega_0)$. Due to the energy conservation law, all integrals in equation (4) can be solved analytically. As a result, one obtains an infinite set of algebraic linear equations for $\tau(\varepsilon)$ which can be written as [6, 7]

$$-A(\varepsilon_m)\tau(\varepsilon_m - \hbar\omega_0) + B(\varepsilon_m)\tau(\varepsilon_m) - C(\varepsilon_m)\tau(\varepsilon_m + \hbar\omega_0) = 1 \quad (6)$$

where $\varepsilon_m = \varepsilon + m\hbar\omega_0$, $0 < \varepsilon \leq \hbar\omega_0$, $m = 0, 1, 2, \dots$. Here A , B , and C are analytical functions of energy, namely, $B(\varepsilon)$ is the total scattering rate from state with energy ε (including the elastic terms described by equation (5)), while $A(\varepsilon)$ and $C(\varepsilon)$ are originated by scatterings into the state ε due to optical phonon absorption and emission, respectively (note that $A = 0$ for $m = 0$). The system is truncated at a sufficiently high energy value $\varepsilon_n \gg \hbar\omega_0$, and is closed by assuming that $\tau(\varepsilon_n \pm \hbar\omega_0) = \tau(\varepsilon_n)$. Then, the solution of the truncated system gives the relaxation time as a function of electron energy. Finally, the static low-field mobility is calculated as

$$\mu_0 \equiv \frac{1}{E} \int v(\mathbf{p}) f(\mathbf{p}) d\mathbf{p} = \frac{e}{3k_B T F} \int v^2(\varepsilon) \tau(\varepsilon) f_0(\varepsilon) g(\varepsilon) d\varepsilon \quad (7)$$

where k_B is the Boltzmann constant, T the lattice temperature, $g(\varepsilon)$ the density of states here considered to be of nonparabolic type, and $F = \int f_0(\varepsilon) g(\varepsilon) d\varepsilon$ a normalization constant. By supposing that $\tau(\varepsilon)$ remains the same when a harmonic electric field $E(t) = E_1 \exp(i\omega t)$ is applied instead of the static one, the harmonic part of the distribution function takes the form

$$f_1(\mathbf{p}, \omega) = \frac{\tau(\varepsilon)}{1 + i\omega\tau(\varepsilon)} e \mathbf{E}_1 \mathbf{v}(\mathbf{p}) \frac{d}{d\varepsilon} f_0(\varepsilon) \quad (8)$$

where i is the imaginary unit. Then, in full analogy with equation (7) the low-field mobility spectrum is calculated as

$$\mu(\omega) = \frac{e}{3k_B T F} \int v^2(\varepsilon) \frac{\tau(\varepsilon) - i\tau^2(\varepsilon)\omega}{1 + \tau^2(\varepsilon)\omega^2} f_0(\varepsilon) g(\varepsilon) d\varepsilon. \quad (9)$$

The static diffusion coefficient is then obtained by using the Einstein relation $D_0 = \mu_0 k_B T / e$ and the spectral density of velocity fluctuations is given by a similar relation:

$$S_{vv}(\omega) = \frac{4k_B T}{e} \text{Re}[\mu(\omega)] \quad (10)$$

where $\text{Re}[\mu(\omega)]$ is the real part of the mobility.

3. Numerical results

As an application, figure 1 reports the relaxation time as a function of the electron energy calculated for a bulk of uncompensated wurtzite GaN at room temperature for three values of the doping level $N_D = 10^{16}$, 10^{17} and 10^{18} cm^{-3} (curves 1–3). For comparison, the dotted curve shows the relaxation time of the polar optical phonon scattering alone. The parameters of the scattering mechanisms and band structure are taken from [9]. Note that the band structure of these materials is well described by the nonparabolic spherically symmetric approximation. As known [6, 7], abrupt discontinuities originated by the polar optical phonon scattering appear at electron energies $\varepsilon = m\hbar\omega_0$. These discontinuities are most pronounced at low values of m and practically disappear for values of m above about 10. With the increase of the doping

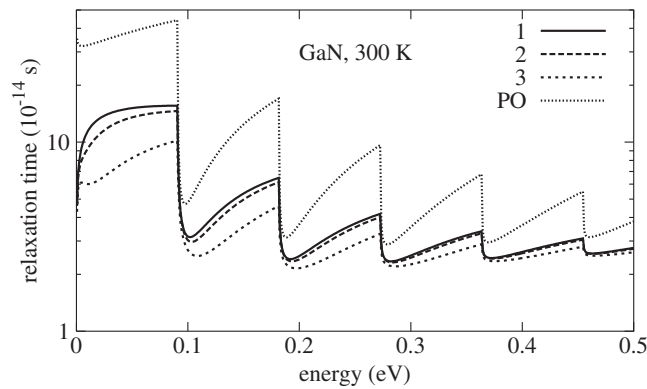


Figure 1. Relaxation time as a function of electron energy for uncompensated wurtzite GaN at different dopings $N_D = 10^{16}$, 10^{17} and 10^{18} cm^{-3} (curves 1–3), and for polar optical phonon scattering alone (PO).

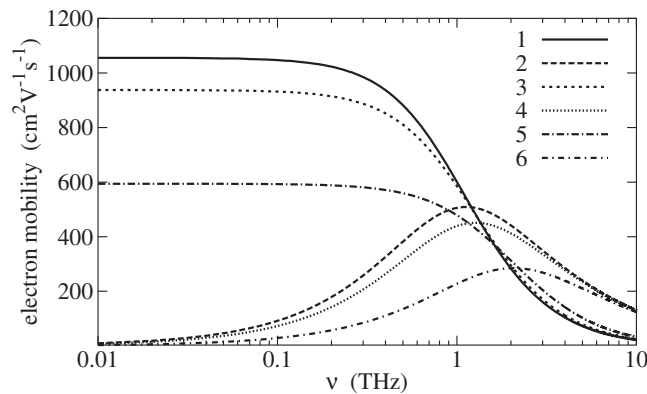


Figure 2. Real (curves 1, 3, 5) and imaginary (curves 2, 4, 6) parts of the low-field mobility as functions of frequency for uncompensated wurtzite GaN at different dopings $N_D = 10^{16}$ (1, 2), 10^{17} (3, 4) and 10^{18} cm^{-3} (5, 6).

level, the most significant reduction of the relaxation time takes place in the low energy region due to the significant increase of the impurity scattering intensity at low carrier velocities.

The frequency dependence of the real and imaginary parts of the low-field mobility calculated in accordance with equation (9) are shown in figure 2. Due to the very short relaxation time, the cut-off of the spectrum practically occurs in the THz region.

Figure 3 reports the mobility associated with the various scattering mechanisms into which the total value of the static mobility can be decomposed as functions of the lattice temperature T . As expected, in the low-temperature region the main contribution comes from impurity scattering, while in the high-temperature region the total mobility is mainly determined by polar optical phonon scattering. The dependence of the electron mobility upon the impurity concentration is presented in figure 4 for wurtzite GaN and InN. Due to a lower effective mass ($m^* = 0.11$ and 0.2 in InN and GaN, respectively) the InN mobility is higher. The electron mobilities presented in figures 3 and 4 are found to agree well with other theoretical results (see, e.g. [1–3]), thus providing a further validation of the present approach.

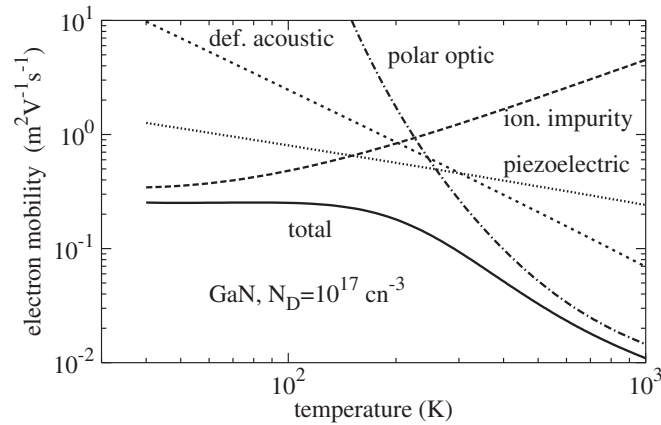


Figure 3. Temperature dependence of the low-frequency total mobility and of separate contributions in which it can be decomposed according to the various scattering mechanisms reported in the figure. Values refer to wurtzite GaN, with $N_D = 10^{17} \text{ cm}^{-3}$.

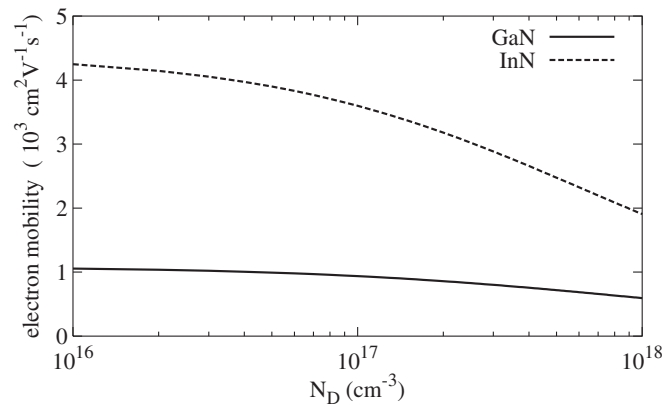


Figure 4. Electron mobility of wurtzite GaN and InN as function of N_D . $T = 300 \text{ K}$.

As we mentioned in the previous section, due to the validity of the Einstein relation at thermal equilibrium, the real part of the mobility can be used to calculate the diffusion coefficient D_0 and, in turn, the spectral density of velocity fluctuations $S_{vv}(\nu)$ (see equation (10)). As an example, figure 5 shows the temperature dependence of the electron diffusivity D_0 at different impurity concentrations N_D for the case of wurtzite GaN. Initially, D_0 increases with T since low-temperature mobility is nearly constant (see the solid curve in figure 3). Then, D_0 reaches a maximum and finally decreases due to the significant decrease of the high-temperature mobility.

The spectral density of velocity fluctuations recalculated from the spectrum of the real part of the mobility is reported as a continuous curve in figure 6. For comparison, the symbols report the result of a direct Monte Carlo simulation performed with the same parameters at a low electric field of $E = 200 \text{ V cm}^{-1}$. The excellent agreement between the two results confirms the validity of the theoretical approach developed here. It should be underlined that by using the average relaxation rate obtained from the static mobility $\nu_0 = e/m^* \mu_0$ one can

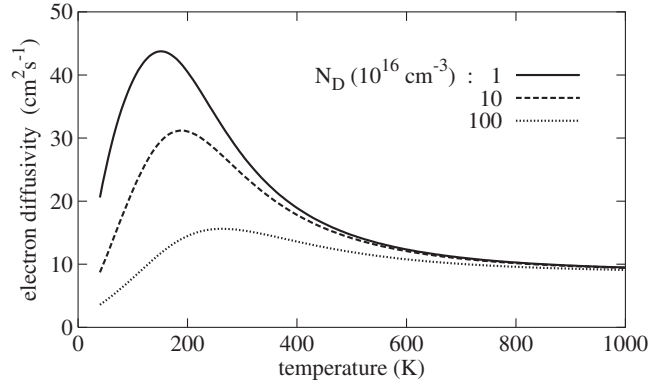


Figure 5. Electron diffusivity of wurtzite GaN as a function of T at different doping levels.

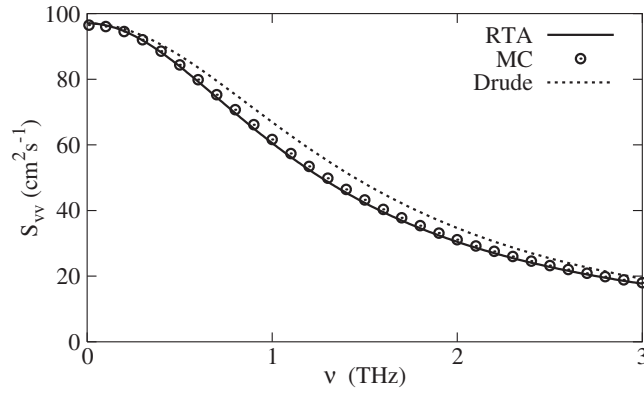


Figure 6. Spectral density of velocity fluctuations calculated by the relaxation-time approach (RTA), directly by the Monte Carlo (MC) method, and by using the Drude approximation given by equation (11). Results refer to GaN at $T = 300$ K, and $N_D = 10^{17}$ cm $^{-3}$.

also calculate the mobility and velocity noise spectra in the framework of the standard Drude approach as

$$\text{Re}[\mu(\omega)] = \frac{\mu_0 v_0^2}{v_0^2 + \omega^2}. \quad (11)$$

The result is presented in figure 6 by the dashed curve. Comparing all three curves presented in figure 6 one can conclude that both RTA and MC results slightly differ from the pure Lorentzian behaviour predicted by equation (11).

To understand the origin of such a discrepancy, figure 7 presents the time dependence of the correlation function of velocity fluctuations for the same case as figure 6. Here, RTA and Drude curves are obtained by the Fourier transform of the spectral density of velocity fluctuations shown in figure 6 (for the Drude approximation, as follows from equation (11), it is simply $C_{vv}(t) = C_{vv}(0) \exp(-v_0 t)$), while the MC curve presents the result of direct MC calculations of the correlation function. As follows from figure 7, indeed, at the initial stage of the $C_{vv}(t)$ decay ($t \leq 0.2$ ps), both RTA and MC curves follow the usual exponential behaviour with v_0 given by the Drude model. However, at longer times the slope of the RTA and MC curves changes, i.e. the relaxation is determined by at least two characteristic times. This is

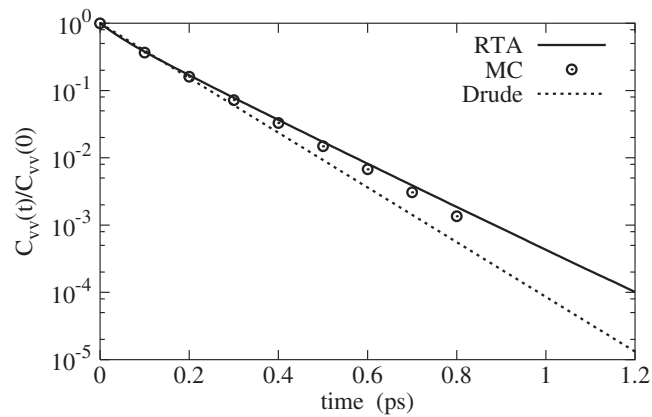


Figure 7. Correlation function of velocity fluctuations calculated for the same conditions as figure 6.

the reason why their spectral densities cannot be rigorously described by a single-Lorentzian decay.

4. Conclusions

We have implemented the calculation of the low-field mobility in compound semiconductors by using the exact solution of the linearized Boltzmann transport equation within the relaxation time approach in a nonparabolic isotropic band model. Numerical calculations are applied to the case of electrons in bulk nitrides, wurtzite GaN and InN at different lattice temperatures and impurity concentrations. The theoretical approach, which is validated by comparison with Monte Carlo simulations, represents a valuable analytical alternative to numerical simulators which are computationally more expensive.

Acknowledgments

The authors wish to acknowledge the financial support of NATO Collaborative Linkage Grant PST.EAP.CLG 980629, the French CNRS position of associated researcher and the Italian Ministry of Education, University and Research (MIUR) under the project 'Noise models and measurements in nanostructures'.

References

- [1] Bhapkar U and Shur M 1997 *J. Appl. Phys.* **82** 1649
- [2] Albrecht J, Wang R, Ruden P, Farahmand M and Brennan K 1998 *J. Appl. Phys.* **83** 4777
- [3] Chin V, Tansley T and Osotchan T 1994 *J. Appl. Phys.* **75** 7365
- [4] Rode D and Gaskill D 1995 *Appl. Phys. Lett.* **66** 1972
- [5] Dhar S and Ghosh S 1999 *J. Appl. Phys.* **86** 2668
- [6] Fletcher K and Butcher P 1972 *J. Phys. C: Solid State Phys.* **5** 212
- [7] Ridley B K 1998 *J. Phys.: Condens. Matter* **10** 6717
- [8] Chattopadhyay D 1980 *J. Appl. Phys.* **51** 1851
- [9] Foutz B, O'Leary S, Shur M and Eastman L 1999 *J. Appl. Phys.* **85** 7727